Skutelsky, E., & Farquhar, M. G. (1976) J. Cell Biol. 71, 218-231.
Spiro, R. G., & Bhoyroo, V. D. (1974) J. Biol. Chem. 249, 5704-5717.
Thomas, D. B., & Winzler, R. J. (1969) J. Biol. Chem. 244, 5943-5946.
Tsuji, T., Tsunehisa, S., Watanabe, Y., Yamamoto, K., Tohyama, H., & Osawa, T. (1983) J. Biol. Chem. 258, 6335-6339.
Van den Eijnden, D. H., Evans, N. A., Codington, J. F., Reinhold, V., Silber, C., & Jeanloz, R. W. (1979) J. Biol. Chem. 254, 12153-12159.
Van Langenhove, A., & Reinhold, V. N. (1985) Carbohydr. Res. 143, 1-20.
Weber, P. (1979) Eleventh International Congress Biochemistry, p 717 (Abstr. 14-7R100).
Weber, P., & Winzler, R. J. (1969) Arch. Biochem. Biophys. 129, 534-538.
Weber, P., & Winzler, R. J. (1970) Arch. Biochem. Biophys. 137, 421-427.
Winzler, R. J., Harris, E. D., Pekas, D. J., Johnson, C. A., & Weber, P. (1967) Biochemistry 6, 2195-2202.
Young, J. D., Tsuchya, D., Sandlin, D. E., & Holroyde, M. J. (1979) Biochemistry 18, 4444-4448.

Self-Association and Active Enzyme Forms of *Naja naja naja* and *Crotalus atrox* Phospholipase A_2 Studied by Analytical Ultracentrifugation†

Thomas Bukowski and David C. Teller*
Department of Biochemistry, University of Washington, Seattle, Washington 98195
Received July 23, 1986

ABSTRACT: The dimerization of phospholipase A_2 ($PLPA_2$) from *Naja naja naja* (Pakistani cobra) and *Crotalus atrox* (Western Diamondback rattlesnake) has been studied from pH 2.5 to 11 at 20 °C in 1 mM $CaCl_2$, 0.21 M ionic strength. For the *C. atrox* enzyme, it was found necessary to use a combination of sedimentation equilibrium and fluorescence yield data to analyze the association. Sedimentation equilibrium in the analytical ultracentrifuge sufficed for the study of the *N. naja* $PLPA_2$. In the region of enzymatic activity at pH 8, the dimerization association constants found were $k_2 = 2.8 \times 10^6$ L/mol and $k_2 = 6.9 \times 10^4$ L/mol for the *C. atrox* and *N. naja* enzymes, respectively. Analytical linked functions are presented which describe the data. Because the associations are linked to Ca^{2+} as well as the hydrogen ion, no attempt was made to interpret the ionization of residues in terms of the molecular structure. Active-enzyme sedimentation velocity experiments have been used to study the relation between enzymatic activity and association for both the *C. atrox* and *N. naja* enzymes. The substrate 1,2-dibutyryl-*sn*-glycero-3-phosphocholine (diC4PC) did not dissociate the *C. atrox* $PLPA_2$. The substrate 1,2-dihexanoyl-*sn*-glycero-3-phosphocholine (diC6PC) at 7.5 mM dissociated the *C. atrox* $PLPA_2$ when monitored either as the active enzyme or as the Sr^{2+}-inhibited enzyme. At low enzyme concentrations, 40 mM diC4PC had no effect on *N. naja* $PLPA_2$ dimerization. However, the sedimentation coefficients observed at enzyme concentrations above 0.2 mg/mL in active-enzyme sedimentation velocity experiments were larger than the values predicted from the thermodynamic studies. Sedimentation coefficients observed for the *N. naja* $PLPA_2$ acting on diC6PC were larger than those of the monomeric protein, which was the form layered on this substrate. The dissociation of the *C. atrox* $PLPA_2$ effected by diC6PC was analyzed by the thermodynamics of association and the kinetic Michaelis constant. The analysis suffices to account for the observed sedimentation coefficient. The sedimentation behavior of the *N. naja* $PLPA_2$ acting on diC6PC substrate was analyzed in terms of a protein–lipid complex. With this model, 68 ± 16 phospholipid molecules per protein monomer were determined. It is proposed that this enzyme has two micelle nucleation sites per monomer. These putative sites promote micelle formation of the substrate on the enzyme below the critical micelle concentration of the lipid alone.

Considerable controversy has been generated over the years concerning the active enzymatic species of the phospholipase A_2 enzymes. At the current time, it is accepted [see review by Verheij et al. (1981)] that *Crotalus adamanteus* phospholipase A_2 hydrolyzes small nonmicellar substrates as the dimeric protein. For the cobra (*Naja*) venom enzymes, a variety of associated states of the protein have been proposed, but the connection between association and activity is by no means clear.

We have been examining the self-association of both the *Crotalus atrox* and *Naja naja naja* phospholipase A_2 enzymes by sedimentation equilibrium in the analytical ultracentrifuge and by fluorescence studies. It is natural for us to be interested in the relation between the dimerization in the absence of substrate and the enzymatic activity of the proteins. The absence of thermodynamic linkage between association and substrate binding, as was found for the saccharide binding by concanavalin A (Senear & Teller, 1981b), would mean that our thermodynamic studies are applicable to the enzymology as well as the protein structure. On the other hand, linkage of the substrate binding and turnover to the dimerization is of direct interest to structure–function relationships of these enzymes.

One particularly puzzling aspect of the enzymology of *Crotalus atrox* phospholipase A_2 is that the enzyme is gen-

† This work was supported by National Institutes of Health Grant GM 13401.

0006-2960/86/0425-8024$01.50/0

erally believed to act as the dimer (Shen et al., 1975; Smith & Wells, 1981), while the crystal structure of the dimer (Keith et al., 1981; Brunie et al., 1985; Renetseder et al., 1985) indicates the active center residues are inaccessible to substrate. The results of the present study afford a partial resolution of this dilemma.

We have used a variety of sedimentation velocity studies to examine the active forms of *Naja* and *Crotalus* phospholipase A_2 at pH 8.2. By monitoring the hydrolysis of synthetic substrates with a pH indicator, we can measure the sedimentation coefficient of a zone of enzyme. In order to verify these active-enzyme sedimentation experiments, we have also examined the sedimentation velocity of the protein in the presence of substrates with the essential calcium ion replaced by strontium.

The results of the experiments indicate that 1,2-dibutyryl-*sn*-glycero-3-phosphocholine (diC4PC)[1] turnover is not thermodynamically linked (or only weakly linked) to the dimerization state of *Naja naja naja* and *Crotalus atrox* phospholipase A_2. 1,2-Dihexanoyl-*sn*-glycero-3-phosphocholine (diC6PC), on the other hand, profoundly influences sedimentation behavior of both enzymes. At 7.5 mM concentration, this substrate induces dissociation of the *Crotalus atrox* phospholipase A_2 dimer. The *Naja naja naja* phospholipase A_2 is converted by this substrate to a more rapidly sedimenting form. These results are discussed with reference to prior studies on the same problem (Shen et al., 1975; Smith & Wells, 1981), recent studies of substrate-induced aggregation of *Naja* phospholipases A_2 (van Eijk et al., 1983; Plückthun & Dennis, 1985), and the energetics of substrate binding.

We propose that the *Naja naja naja* enzyme acts as a nucleation center for the formation of two micelles of diC6PC per phospholipase A_2 monomer at substrate concentrations below the critical micelle concentration. By extension of this proposal to other compounds, several enzyme properties previously reported by others become clearer.

Materials and Methods

Materials

Lyophilized snake venoms were purchased from the Miami Serpentarium, Miami, FL. *Crotalus atrox* phospholipase A_2 ($PLPA_2$) was purified from venom lots CX12KZ and CX9S6BZ; the venom lots for *Naja naja naja* $PLPA_2$ enzyme purification were NP13SZ and NNP0SZ.

Lactic acid dehydrogenase (LDH) from halibut muscle was a gift of Dr. Sidney Bernhard. Trypsin (lot 34J6168) was purchased from Cooper Biomedical with a specific activity of 195 units/mg. Porcine pancreatic prophospholipase A_2, 35 units/mg, lot 405138, was purchased from Calbiochem.

Benzoylarginine ethyl ester (BAEE) (lot 110187) and pyruvate (lot 410013) were purchased from Calbiochem. The disodium salt of NADH was grade III from Sigma. Phenol Red was lot 440625 from Coleman and Bell, and Cresol Red was Sigma lot C-9877.

For the synthesis of phosphatidylcholine substrates, the following chemicals were employed. Hexanoic acid and trifluoroacetic acid were products of Aldrich Chemical Co, as was the 99% trifluoroacetic anhydride. This last compound was taken from previously unopened bottles. L-α-Glycerophosphorylcholine, grade I, was purchased from Sigma as the cadmium chloride complex which was desalted on mixed-bed Biorex 70/AG3-X4A prior to being dried over P_2O_5.

All other chemicals were analytical grade or the finest available.

Methods

Chemical Methods. (*A*) *Purification of Phospholipase A_2.* The *Naja naja naja* $PLPA_2$ purification was carried out by the procedure of Wells (1975) with only slight modification. We employed 45% 2-propanol fractionation and performed the DE-52 cellulose (Whatman) chromatography in 5 mM potassium phosphate buffer developed with an exponential gradient from 0.04 to 0.28 M KCl at pH 7.0. Only the major isozyme eluting second in the chromatography at 0.25 M KCl was used in these studies. This protein was homogeneous by SDS disc gel electrophoresis. The specific activity was 5500 μmol min^{-1} mg^{-1} in the lipoprotein assay (de Haas et al., 1968). In analytical sedimentation equilibrium studies, the enzyme behaves as a single thermodynamic system at all pHs, pCa's, and temperatures studied in over 200 experiments (T. Bukowski and D. C. Teller, unpublished results). The extinction coefficient employed for protein concentration measurements was $E^{1\%}_{280nm} = 22.0$ (Darke et al., 1980).

Crotalus atrox $PLPA_2$ was purified by the procedure of Wells (1975) with no modification. It was homogeneous in overloaded SDS disc gels. The specific activity was 2900 μmol min^{-1} mg^{-1} in the lipoprotein assay (de Haas et al., 1968). This enzyme is also a single thermodynamic system of monomers and dimers in the pH ranges 2–4 and 9–11 in 1 mM $CaCl_2$, 0.21 M ionic strength. The extinction coefficient employed was $E^{1\%}_{280nm} = 22.7$ (Wells & Hanahan, 1969).

(*B*) *Synthetic Substrate Synthesis.* 1,2-Dibutyryl-*sn*-glycero-3-phosphocholine (diC4PC) and 1,2-dihexanoyl-*sn*-glycero-3-phosphocholine (diC6PC) were synthesized by the procedure reported by Kanda and Wells (1981). Purity of the products was monitored by thin-layer chromatography (Kanda & Wells, 1981). The compounds were stored in dry methanol at −20 °C. The concentration of this stock solution was determined by phosphate analysis (Fiske & Subbarow, 1929). Prior to use, an aliquot of the stock solution was dried and made to volume for the experiments. Monohydrate molecular weights were employed for concentration calculations.

(*C*) *Enzyme Assays.* The LDH assay which monitored NADH at 340 nm was that of Kornberg (1955). The indicator assay of this enzyme was that of Kemper and Everse (1973) utilizing 0.1 mM Tris-HCl with 0.0014% Phenol Red indicator, pH 6.5 at 20 °C, monitored at 560 nm.

The trypsin indicator assay consisted of 10 mM BAEE, 10 mM $CaCl_2$, 0.2 M NaCl, 0.1 mM Tris-HCl, and 0.0014% Phenol Red indicator, pH 8.1 at 20 °C, monitored at 560 nm. Linearity of the absorbance change with trypsin concentration was verified.

The egg yolk lipoprotein assay of de Haas et al. (1968) was employed as a pH-stat assay of phospholipases A_2.

The spectrophotometric assay mixture for $PLPA_2$ enzymes contained 0.1–0.2 M NaCl or KCl, 1 mM $CaCl_2$, 0.0014% Cresol Red indicator, variable glycylglycine buffer (to regulate the sensitivity), and an amount of 2-(*N*-morpholino)ethanesulfonate (MES) equal to the glycylglycine, pH 8.2–8.5. The MES buffer prevents the solution from becoming too acid and producing an artifact in the ultracentrifuge results. The substrate concentration for diC4PC was 40 mM. The sub-

[1] Abbreviations: $PLPA_2$, phospholipase A_2; LDH, lactic acid dehydrogenase; BAEE, benzoylarginine ethyl ester; diC4PC, 1,2-dibutyryl-*sn*-glycero-3-phosphocholine; diC6PC, 1,2-dihexanoyl-*sn*-glycero-3-phosphocholine; MES, 2-(*N*-morpholino)ethanesulfonic acid; cmc, critical micelle concentration; SDS, sodium dodecyl sulfate; Tris-HCl, tris(hydroxymethyl)aminomethane hydrochloride. We use lower case *k*'s as association constants and upper case *K*'s as dissociation constants; the exception is K_2, which represents $2k_2/M_1$, the association dimerization constant in liters per gram units.

strate concentration principally used for diC6PC was 7.5 mM. The Cresol Red was monitored at 570 nm, with the absorbance at 440 nm used for pH calculations. In the ultracentrifuge, a base-line absorbance scan at 650 nm was subtracted from the 570- and 440-nm scans for pH calculations as a function of radial distance.

In the spectrophotometer, the linearity of the assay with enzyme concentration using 40 mM diC4PC was excellent, although some difficulties were encountered with spontaneous hydrolysis limiting the sensitivity to 0.5 mM and above in glycylglycine–MES concentration. Hydrolysis of 7.5 mM diC6PC was also linear with enzyme concentration but with a small negative intercept. The absorbance was not linear with time in the initial time region which may be related to the nonzero intercept.

From spectrophotometric measurements and pH measurements of the same solutions of the assay mixture without substrate, we determined (by least squares) the empirical equation for the pH of Cresol Red solutions:

$$\mathrm{pH} = 8.214 - \log [(18.45 - R)/(6.742R - 0.210)] \quad (1)$$

where R is the ratio of 570- to 440-nm absorbance. This equation is accurate to ±0.1 pH unit in the temperature range of 20–22.5 °C and pH 7.2–9.2.

Ultracentrifuge Methods. High-speed sedimentation equilibrium experiments using the Rayleigh interference optics were performed essentially as described by Teller (1973). Solutions were dialyzed overnight prior to the experiments, and the dilutions were made by using dialysate for filling the Yphantis (1964) six-channel centerpiece. Photographic plates were read and processed as described by Senear and Teller (1981a). Equilibrium constants for the monomer–dimer equilibrium were calculated from the number-, weight-, and z-average molecular weights as described by Hoagland and Teller (1969).

The partial specific volumes of *Crotalus* and *Naja* $PLPA_2$ enzymes were determined by fitting the molecular weight distributions in sedimentation equilibrium experiments to a monomer–dimer system with the analytical molecular weights of 13 679 g/mol for *Crotalus* $PLPA_2$ and 13 441 g/mol for *Naja* $PLPA_2$ (Senear & Teller, 1981b). The values found were 0.6779 mL/g for *Naja* $PLPA_2$ and 0.7121 mL/g for *Crotalus* $PLPA_2$ at 20 °C. Densities and viscosities were calculated from International Critical Tables, 1926–1933 or Landoldt-Börnstein (1977) or were measured. Density measurements were made in a 1.37-mL pycnometer. Viscosity measurements were performed on 3 mL of solvent in an Ostwald viscometer with a Hewlett-Packard (Mechrolab) 5901 viscometer timer. The water bath for these measurements was controlled to ±0.02 °C.

Moving-boundary sedimentation velocity experiments were performed in double-sector 12-mm aluminum-filled epoxy centerpieces and monitored at 280 nm with a Beckman scanner modified as described by Teller (1973). Data were collected in a PDP-12 computer, and the boundary was analyzed for s and D by using Faxén's (1936) solution to the Lamm (1929) equation reported by Fujita (1975, eq 2.127, p 80) but with the sign reversed for the error function integral. These calculations for the least-squares fit to s and D were performed on a VAX 11/780 computer.

Zone sedimentation velocity experiments were performed by layering 10 μL (range 5–20 μL) of enzyme solution in dilute buffer on 0.30–0.32 mL of solvent containing 0.2 M KCl for density stabilization. The centerpieces used were constructed from standard 12-mm aluminum-filled epoxy centerpieces by drilling a small, slanted hole in the centerpiece and scratching a horizontal scribe line from the centrifugal position of the hole to the sector. The solution layered at approximately 6000 rpm. The 280-nm absorbance data were collected and analyzed in the PDP-12 computer. The peak maximum and point of zero derivative were used to calculate the sedimentation coefficients.

Active-enzyme sedimentation velocity experiments were performed in the same cells as the zone experiments, and data collection was also the same, except the scan wavelengths differed from enzyme to enzyme. Scans were taken at 4-min intervals (2 min for LDH).

In the active-enzyme sedimentation velocity method (Cohen, 1963; Cohen & Mire, 1971), one layers the enzyme as a zone on a suitable substrate solution. As the zone sediments, the absorbance of the substrate solution is recorded at fixed time intervals. The absorbance profile at each time t is subtracted from that at $t + \Delta t$, resulting in a nearly Gaussian distribution of absorbance difference. Let the position of the maximum in the ΔA profile be r^*; then the sedimentation coefficient of the active enzyme is determined from the slope, $s\omega^2 = \mathrm{d} \ln r^*/dt$. One can also measure the r^* position from the zero position of $(\partial \Delta A/\partial r)_t$ or the equivalent zone position of Holcenberg et al. (1972).

In the active-enzyme experiments, the equivalent zone position (Holcenberg et al., 1972) and also the peak maximum and zero-derivative positions were determined; however, the sedimentation coefficients determined from the equivalent zone positions were often different than the other two for pH-linked assays. Only the sedimentation coefficients determined from the peak maximum and zero-derivative positions are reported here. In this work, no dependence of sedimentation coefficient on the time interval between absorbance profile differences was observed.

In the case of a proton-linked assay where an indicator is used, one is removed by one step from the enzymatic reaction. The pH of the solution occupied by the enzyme zone is variable. Depending on the variation of enzymatic activity with pH and the pH change in the zone, observed sedimentation coefficients may be artifactually increased. When enzyme activity is higher in the leading part of the zone, diffusional spreading of the zone biases the measurement toward the leading portion of the zone, resulting in too large an estimate of the sedimentation coefficient. The problem is particularly insidious because the effect may be only a few percent increase in s. It can be detected and avoided by variation of the enzyme loading over a broad range and by spectrophotometric measurement of the solution pH.

Fluorescence Measurements. Fluorescence measurements on *Crotalus* $PLPA_2$ were carried out by using Aminco Model SPF-500 and Perkin-Elmer Model MPF-44A spectrofluorometers. The excitation wavelength was 292 nm, and emission was measured at 340 nm. The band-pass was 5 nm for both excitation and emission wavelengths. Temperature was controlled with a circulating water bath, and 5–15 min was allowed for temperature equilibration.

Calculation of Crotalus Dimerization Equilibrium Constants. Fluorescence yield data could be analyzed to determine the dimerization constants. For this calculation, it was necessary to determine the fluorescence yield of monomer and of dimer. Then from the total fluorescence at a particular concentration, the mole fraction of monomer could be calculated. This was converted to the weight fraction and the equilibrium constant calculated because simple relations exist among the weight fraction, weight/volume concentration, and the dimerization association constant.

To determine the fluorescence yield of monomer and of dimer, both fluorescence and ultracentrifuge data were collected over the same pH range. Since the dimerization association constant, k_2, was known from the ultracentrifuge experiments, the amounts of monomer and dimer were calculated from the total concentration in the fluorescence experiments. Then the fluorescence yields of monomer and of dimer were determined by least-squares fit to the total fluorescence over the short pH region. The fluorescence data were collected over the concentration range of protein from 0.004 to 0.096 mg/mL, so it was necessary in the calculation to account for the quenching of the fluorescence due to absorption of the exciting light.

The detailed calculation was the following. The observed fluorescence yield is given by

$$F = Q(A_1x_1 + A_2x_2) \quad (2)$$

where $Q = 1 - e^{-Bc}$ is the quenching term, A_i is the fluorescence yield, x_i is the mole fraction of monomer or dimer, and c is the total concentration of monomers and dimers in milligrams per milliliter. The extinction parameter, B, was measured with tryptophan and protein solutions as 2.906 mL/mg for these experiments. The fluorescence and ultracentrifuge studies were performed at temperatures between 5 and 35 °C. The A_i and B parameters were temperature independent. The weight fraction of monomer was calculated from the quadratic equation

$$w_1 = [(4K_2c + 1)^{1/2} - 1]/2K_2c \quad (3)$$

where the grams per liter association constant for monomer to dimer, K_2, is $2k_2/M_1$. The mole fraction of monomer was calculated from the weight fraction as

$$x_1 = 2w_1/(1 + w_1) \quad (4)$$

To employ the k_2 values determined by ultracentrifugation at the pH of the fluorescence experiment in the low-pH region, the smooth function was used:

$$\ln k_2 = \mathrm{Cst} - n \ln (1 + k_H H) \quad (5)$$

where k_H is the association constant of thermodynamically linked protons to $n/2$ ionizing residues in the monomer and H is the hydrogen ion concentration. The temperature dependencies utilized were

$$\mathrm{Cst} = a_0 + a_1(1/T - 1/273.15) \quad (6)$$

and

$$pK_H = b_0 + b_1(1/T - 1/273.15) \quad (7)$$

In eq 6 and 7, T is the absolute temperature, and pK_H is log k_H. The parameters fitted to the data consisted of the a_i, b_i, and n of eq 5.

For the fluorescence data series collected at high pH (6–11), ultracentrifuge data from pH 9 to 10.5 were used in a similar calibration, although these were taken only at 20 °C rather than multiple temperatures. Also, eq 5 could not be used as such because the high-pH limit (Cst = ln $k_{2,\nu=0}$) does not exist. Addition of the term $n \ln k_H H$ to eq 5 converted it to the form appropriate for the high-pH part of the association. The Cst term now has the meaning of ln $k_{2,\nu=n/2}$.

With the assumption that the fluorescence yield parameters were pH independent, the fluorescence–dilution experiments at the pH values outside the calibration range were used to compute the equilibrium constant. This calculation was made by simply using eq 2–4 in the reverse of the calibration procedure with the known fluorescence yield parameters, A_i. If log k_2 was significantly correlated with concentration at a particular pH, a straight line was used to extrapolate the value of log k_2 to infinite dilution. The consistency of the assumption of constant fluorescence yield was checked by performing ultracentrifuge experiments from pH 2.3 to 4 and using these values of k_2 to calibrate fluorescence experiments to pH 7.5. Ultracentrifuge experiments from pH 9.5–11 for k_2 were used for calibration of the fluorescence experiments from pH 10.5 down to pH 6. The splining of the two determinations of k_2 from the low-pH and from the high-pH calibration experiments was within a factor of 3 for k_2 in the overlap of pH 6–7.5. For the results reported here, the splining was refined by assignment of the k_2 values to the pH range of 6–7.5 as well as 9–11 for the high-pH (7.5–10.5) fluorescence yield parameter determination.

Error estimates for log k_2 were determined in the following "bootstrap" fashion (Efron & Diaconis, 1983). The calibrating ultracentrifuge experiments were selected randomly with replacement, and the linkage function (eq 5) was fitted to the data. This was repeated 100 times to produce 100 sets of calibrating equations for k_2. At each pH, six points of enzyme dilution were measured in fluorescence. For each ultracentrifuge calibrating equation, the fluorescence data were selected randomly with replacement 10 times, and the fluorescence yield parameters were calculated. These yield parameters were used to compute log k_2 from the similarly randomly selected fluorescence data. The standard errors from the mean of these randomized data were taken as the experimental errors for the values of the observed log k_2. The mean values of randomized log k_2 were very close to the experimentally determined values. The reason this rather elaborate error analysis was performed was the errors determined by model-dependent statistical methods were very much smaller than expected. This bootstrap procedure yielded error estimates more in line with our expectation.

Results

Dimerization of Crotalus and Naja Phospholipase A_2. The very strong association of protomers in the dimer of *Crotalus* phospholipase A_2 precluded the determination of the association constants by sedimentation equilibrium in the ultracentrifuge between pH 4 and 9. For this reason, the nonlinearity of the fluorescence yield was analyzed in terms of the monomer–dimer equilibrium (Wells, 1971). The results of this analysis are presented in Figure 1. The utility of these data is to estimate the energy changes involved in the binding of substrate diC6PC in order to dissociate the dimer.

To obtain a smooth function which would describe the data of Figure 1, we have analyzed the data using linked functions (Wyman, 1964) together with nonlinear least-squares fitting of the data to a postulated reaction scheme. The elementary reaction cycles are assembled in a generating function (Szabo & Karplus, 1972, 1976; Lee & Karplus, 1983). Since the data of Figure 1 do not asymptote to a fixed constant either at very low pH or at very high pH, the appropriate fitting function for a symmetric dimer formed of two monomers is

$$\log k_{2,\mathrm{obsd}} = \log k_{2,\nu=1} + 2 \log (k_{1,\mathrm{M}}H) - 2 \log (1 + k_{1,\mathrm{M}}H) - 2 \log (1 + k_{n,\mathrm{M}}H) + \sum_i 2 \log (1 + k_{i,\mathrm{D}}H)/(1 + k_{i,\mathrm{M}}H) \quad (8)$$

The symbol $k_{2,\mathrm{obsd}}$ represents the observed association constant at a particular pH, and $k_{2,\nu=1}$ is the association constant from monomer to dimer for the monomeric species which has one linked proton bound and can dimerize. In eq 8, it is considered that there are n ionizable groups in the monomer ordered from highest, $pK_{1,\mathrm{M}}$, to lowest, $pK_{n,\mathrm{M}}$. The sum over i is from 2 to $n - 1$ for the residues in the monomer which shift pK between monomeric, M, and dimeric, D, states. In

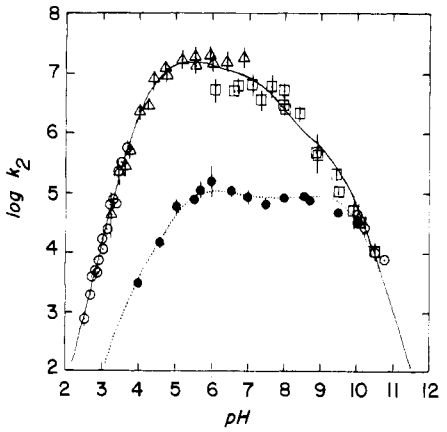

FIGURE 1: Dimerization of *Crotalus* and *Naja* venom $PLPA_2$ enzymes as a function of pH at 20 °C in 1 mM $CaCl_2$, 0.21 M ionic strength. The open symbols represent the *Crotalus* dimerization data, and the solid line is drawn for the least-squares fit to eq 8 and Scheme I of the text. The closed symbols depict the *Naja* dimerization data, and the dotted line was obtained by using eq 8 and Scheme II as described in the text. The symbols have the following meaning: Circles represent data obtained from sedimentation equilibrium experiments, triangles are from fluorescence experiments calibrated by the low-pH ultracentrifuge data, and squares are from fluorescence experiments calibrated by the high-pH ultracentrifuge data and the low-pH calibrated fluorescence data in the region of overlap.

Scheme I: *Crotalus* $PLPA_2$ Dimerization

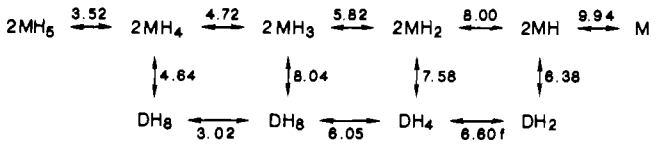

Schemes I and II below, $n = 5$, $pK_{5,M}$ is that for the proton dissociation of MH_5, and $pK_{1,M}$ is that for proton dissociation of MH.

Scheme I presents the parameters found which fit the *Crotalus* $PLPA_2$ together with the model used for the linkage of pH and dimerization. It was found necessary to assume that the dimer is symmetric in order to fit the data. This assumption is only partly correct. In the crystal structure in the absence of Ca^{2+} at low pH, the dimer does not have exact symmetry (Keith et al., 1981). We have performed a pH titration of the deuteriated enzyme in the 500-MHz NMR apparatus (Bruker WM-500) of Dr. Brian Reid in 1 mM $CaCl_2$, 0.21 M ionic strength at 20 °C. This experiment (data not shown) performed by Dr. Dennis Hare yielded a doubled resonance for the histidyl residue we have assigned as His-34. We have not been able to find a resonance peak corresponding to His-48; a similar circumstance has been reported for the pancreatic enzymes (Aguiar et al., 1979). The His-34 doublet resonance titrated with $pK^* = 8.9$ and within experimental error was the same for both peaks of the doublet, consistent with local asymmetry. This high pK^* for His-34 is not at variance with the formation of a salt link to Glu-6 in the crystal structure in the absence of Ca^{2+}, however (Renetseder et al., 1985).

The horizontal numbers in Scheme I give the pK's of linked residues while the vertical numbers are log k_2 values for the association of monomer to dimer. The numbers of linked protons on each species are given. The character f following the pK of 8.6 indicates this parameter was held fixed in the least-squares fit to the data. The reactions shown in Scheme I are not completely realistic since a pK of 8.0 must be assigned to His-34 in the monomer. One would expect this residue to be normalized in the monomer. Apart from the obvious

Scheme II: *Naja* $PLPA_2$ Dimerization

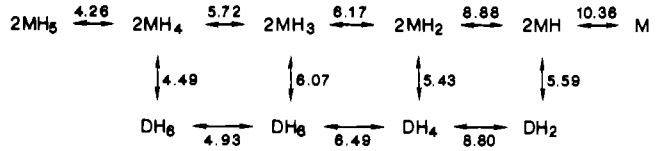

carboxylate ionizations, it is very difficult to assign the pK's to residues. The association is probably linked to Ca^{2+} as is the case for *Naja* $PLPA_2$, and a similar fit to the *Naja* data without accounting for the Ca^{2+} binding is somewhat misleading when compared to the complete model.

Also presented in Figure 1 are the association constants obtained for *Naja* $PLPA_2$ association in 1 mM $CaCl_2$, 0.21 M ionic strength, and 20 °C. These data were obtained entirely by ultracentrifugation and are reliable; that is, they may be regarded as true equilibrium constants. They are part of a larger study in progress in this laboratory. Because of the larger data set (with variable $CaCl_2$ concentrations) and data at other temperatures, we have been able to fit the data to a model as shown by the dotted line in Figure 1. The model (T. Bukowski and D. C. Teller, unpublished results) involves linkage of the dimer formation to binding of Ca^{2+} as well as H^+. In order to compare the *Crotalus* $PLPA_2$ dimerization with that of *Naja*, we have used our current model for dimerization to predict the dotted line of Figure 1 and then treated these idealized data in the same fashion as the *Crotalus* data. Scheme II is the result of this calculation.

In this scheme, the pK's must be regarded as apparent rather than real. The error of Scheme II is in the assumption of dimeric symmetry because there is good evidence the dimer of this enzyme is asymmetric. It forms trimers when the Ca^{2+} concentration is below 1 mM, and the association dependence on Ca^{2+} ion concentration is different in the two protomers of the dimer (T. Bukowski and D. C. Teller, unpublished results). In the order of increasing pK for the monomers, our model includes Asp-99, Asp-49, His-48, Asn-1, and Tyr-52 or Tyr-71. In contrast to Scheme II, the pK's of the complete model are more in line with accepted values or can be rationalized in terms of the known $PLPA_2$ structures (Renetseder et al., 1985; Dijkstra et al., 1981, 1983).

The utility of the data in Figure 1 and the models in Schemes I and II is for the calculation of the amount of monomer and dimer at any desired pH as long as the Ca^{2+} concentration is 1 mM and the ionic strength 0.21 M. The temperature dependence of the *Naja* $PLPA_2$ association is virtually zero in the region of pH 6–9, so the results are of use beyond the 20 °C temperature point. The *Crotalus* $PLPA_2$ association constants must be regarded as estimates of the magnitude of log k_2 rather than established values—they are subject to the assumption of constant fluorescence yield with pH.

Active-Enzyme Sedimentation Velocity with pH Indicator Linked Assays. Table I summarizes the results of these studies. We have found that there are many artifacts that occur in the use of enzyme assays in the analytical ultracentrifuge when proton absorption or release is monitored by a change in the light absorption of a pH indicator. In order to establish that the sedimentation coefficient of phospholipase A_2 could be accurately measured, we have performed several control experiments.

The results of Table I for halibut muscle lactic acid dehydrogenase indicate that the active-enzyme sedimentation obtained by monitoring NADH agrees well with moving-boundary results from the literature (Holbrook et al., 1975). Further, the pH indicator assay of Kemper and Everse (1973)

Table I: Experimental and Theoretical Sedimentation Coefficients

enzyme/substrate	sedimentation coefficient (S) moving boundary	active enzyme	theoretical[a]
lactic acid dehydrogenase	7.36 ± 0.06[b]	7.44 ± 0.05[c]	
		7.44 ± 0.08[d]	
trypsin	[e]	2.51 ± 0.07	2.54
porcine prophospholipase A_2	1.97 ± 0.05		1.98
Crotalus atrox $PLPA_2$	2.94 ± 0.07		1.98, 2.80[f]
diC6PC		2.43 ± 0.13[g]	
Sr, diC6PC–zone	2.48 ± 0.11[h]		
Sr–zone	2.85 ± 0.11		
diC4PC		2.77 ± 0.12	
Naja naja $PLPA_2$			1.98, 2.80
diC4PC		Figure 4[i]	Figure 4[i]
diC6PC		2.40 ± 0.14	
diC6PC (4 mM)		4.68 ± 0.06[j]	

[a] Theoretical sedimentation coefficients are computed from the atomic coordinates by the method of Teller et al. (1979) using the preaveraged tensor of de Haën et al. (1983). [b] Average of several LDH species from Holbrook et al. (1975). [c] NADH/NAD^+ (Kornberg, 1955) assay monitored at 340 nm. [d] LDH proton assay of Kemper and Everse (1973) monitored at 560 nm. [e] Our trypsin preparation was heterogeneous in moving-boundary experiments. [f] Theoretical sedimentation coefficent of monomer and dimer from $s(d) = 1.4s(m)$ (Swanson et al., 1980), where $s(m)$ was taken as the pancreatic $PLPA_2$ value. [g] The values of $s_{20,w}$ were negatively correlated with the experimental temperature: $s_{20,w} = 2.46 - 0.035(T - 20)$. [h] The $PLPA_2$ was preincubated with 10 mM $SrCl_2$ and 7.5 mM diC6PC. 5–20 μL of a 0.45 mg/mL sample of this enzyme was layered on the assay solution without indicator and with 1 mM $CaCl_2$ replaced by 50 mM $SrCl_2$. The protein zone was monitored at 280 nm. For the control experiment in the next row, diC6PC was omitted. [i] Figure 4 presents the variation of active-enzyme sedimentation coefficient with layered concentration of enzyme. [j] For this experiment with diC6PC, the substrate concentration was 4 mM; all other diC6PC experiments in the table utilized 7.5 mM substrate.

yielded an accurate sedimentation coefficient for this enzyme. However, we desired an assay based on the principal of Darrow and Colowick (1962) wherein the indicator is chosen with the same p*K* as the buffer so that the sensitivity can be varied by variation of the buffer concentration. When Cresol Red and glycylglycine were used for LDH in the pH region near 7.5, sedimentation coefficients obtained were uniformly high. In the NADH to NAD^+ assay, the pH rises and the enzyme velocity decreases sharply above pH 8 (Schwert et al., 1967). The decreased enzyme activity in the trailing region of the enzyme zone led to an artifactually increased sedimentation coefficient in these experiments.

Llewellyn and Smith (1978) simulated the active sedimentation method and concluded that the sedimentation coefficient of small enzymes would be artificially raised. We have experimentally tested this conclusion with trypsin hydrolysis of BAEE. It is clear from the trypsin result of Table I that we obtain the same sedimentation coefficient from the active-enzyme method as may be calculated from the atomic coordinates.

A second test of the correspondence of the calculated and observed sedimentation coefficients is provided by the result for porcine pancreatic prophospholipase A_2 of Table I. Moving-boundary experiments agree precisely with that calculated from the porcine $PLPA_2$ coordinate data of Dijkstra et al. (1983).

The active-enzyme sedimentation studies of venom phospholipases were rather confusing to us until we began spectrophotometric measurements of the pH at the beginning and end of the ultracentrifuge experiment (eq 1). We found the result of Smith and Wells (1981) of 2.8 S for *Crotalus* $PLPA_2$ with diC6PC substrate on some occasions, but, in general, the results were quite variable when buffer concentration and

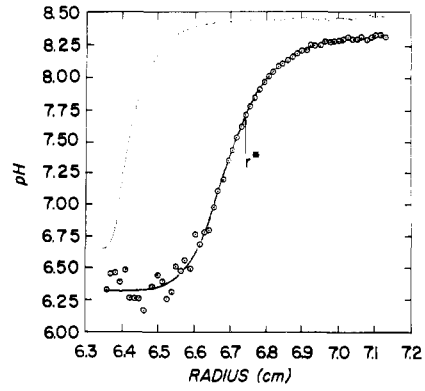

FIGURE 2: Radial pH distribution in active-enzyme sedimentation velocity experiments determined from absorbance at 570 and 440 nm by using eq 1. In this experiment, MES buffer was omitted from the assay mixture to illustrate the low pH encountered by the trailing portion of the enzyme zone. The assay mixture consisted of 0.1 M KCl, 1 mM $CaCl_2$, 7.5 mM diC6PC, 0.5 mM glycylglycine buffer, and 0.0014% Cresol Red. Five microliters of 5 μg/mL *Crotalus* $PLPA_2$ was layered on the substrate solution. The dotted line is the distribution obtained at 0 min at 60 000 rpm. The circles with the hand-drawn solid line are taken from absorbance scans at 60 min at 60 000 rpm. The point marked r^* is the position of the maximum ordinate obtained by subtraction of the 60-min 570-nm absorbance scan from that at 52 min.

enzyme amounts were changed. With the measurement of the solution pH as a function of radial distance in the cell, it became clear that a lack of buffering capacity of the substrate solutions below pH 7 was responsible for the irreproducible results. The situation was rectified by incorporation of MES buffer equal in concentration to the glycylglycine buffer in the substrate solutions. With this modified assay mixture, we obtained reproducible results for the active-enzyme sedimentation.

Figure 2 shows the pH profile of an active-enzyme sedimentation experiment with no low-pH buffering capacity, demonstrating that artificially high sedimentation coefficients were obtained due to lowered enzyme activity in the trailing portion of the enzyme zone. In this experiment, the sedimentation coefficient was calculated to be $s_{20,w} = 2.83 \pm 0.04$ S, in line with the report of Smith and Wells (1981). The position of the r^* position is marked on the pH profile for the scans at 60 min at 60 000 rpm.

Figure 3 is a more complete documentation of the absorbance and pH distribution found with the same amount of enzyme as Figure 2 but with low-pH buffer capacity provided by MES. This sedimentation coefficient was measured as 2.52 ± 0.04 S when corrected to 20 °C in water. This number is one of the many averaged in Table I; the average was 2.43 ± 0.13 S. The average result indicates the weight fraction of dimer was 0.55 ± 0.16 in these active-enzyme experiments. We cannot conclude that the active species of enzyme is the dimer but only that the enzyme zone sediments in a partly dissociated state.

As further verification that the *Crotalus* $PLPA_2$ is dissociated by the diC6PC substrate, we have performed zone sedimentation velocity experiments at 0.45 mg/mL using 50 mM Sr^{2+} to replace Ca^{2+} so that substrate turnover was very slow. For these experiments, the enzyme was preincubated with Sr^{2+} or with Sr^{2+} and diC6PC prior to the sedimentation experiment. The result shown in Table I demonstrates that Sr^{2+} alone has little or no effect on the dimer, but in combination with the diC6PC substrate, the weight fraction of dimeric enzyme is 0.61 ± 0.13.

The dimer equilibrium of the *Crotalus* $PLPA_2$ is not significantly perturbed by diC4PC (Table I). The sedimentation

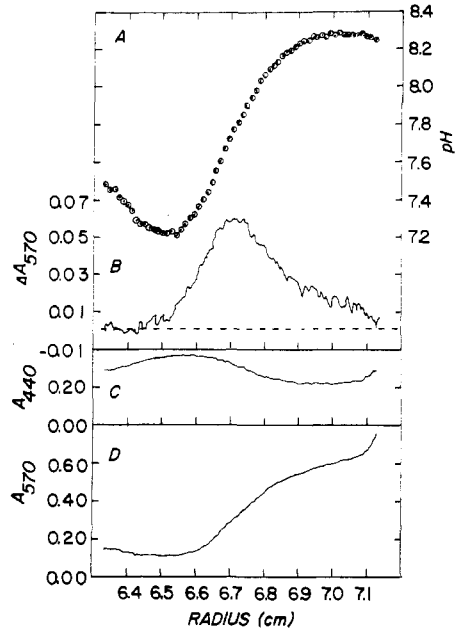

FIGURE 3: Absorbance and pH radial distributions in a doubly buffered active-enzyme sedimentation velocity experiment. The assay conditions were identical with those in Figure 2 except 0.5 mM MES buffer was included in the substrate solution. Ten microliters of 2.5 μg/mL *Crotalus* $PLPA_2$ was layered on the substrate solution, the same total amount of enzyme as in Figure 2. (A) pH distribution at 72–74 min at 60 000 rpm (right ordinate scale). (B) Absorbance difference at 570 nm, 64–72 min. (C) Absorbance at 440 nm and 74 min. (D) Absorbance at 570 nm and 72 min. The absorbance scale is arbitrary and does not correspond to absorbance in a 1-cm path, although it is proportional to it. Scans of panels C and D together with a base-line scan at 650 nm were used to calculate the pH of panel A. The pH drop from the meniscus to the zone of activity is not usual. Note that although the "plateau" of absorbance at 570 nm is lost at the base of the cell, the pH is essentially constant.

coefficient of this enzyme activity is virtually identical with both the theoretical value for the dimer and that observed by moving-boundary sedimentation velocity.

The sedimentation coefficient of *Naja* $PLPA_2$ as a function of concentration of enzyme is shown in Figure 4. This figure demonstrates that the thermodynamically determined equilibrium constant suffices to describe the sedimentation coefficient of the activity of *Naja* $PLPA_2$ to 30% dimer (2.25 S). When the total concentration of $PLPA_2$ is sufficiently large so that the weight fraction of dimer exceeds 0.5, then the sedimentation coefficient of the activity rises above the expected values. The possibility of an artifact must be considered. To shift the pH from 8.2 to 7.2 requires substrate hydrolysis of approximately 0.4 times the total glycylglycine buffer concentration. Such a pH shift corresponds to 80% reduction of the 570-nm absorbance of Cresol Red—larger than we generally accept as a valid experiment. At an enzyme concentration of 0.3 mg/mL, we used 5 mM buffer, so 5% or less of the substrate was hydrolyzed for this point in Figure 4. The highest concentration points of Figure 4 at 0.9 and 1.2 mg/mL $PLPA_2$ utilized 15 and 20 mM buffer, respectively. Only for these two points was more than 10% of the substrate potentially hydrolyzed with consequent possibilities of a nonlinear enzyme assay. Thus, there is no reason to suspect that the increased sedimentation coefficients at and above 0.1 mg/mL in Figure 4 are artificially high.

Table I shows that with the diC6PC substrate the sedimentation coefficient of *Naja* $PLPA_2$ has increased significantly although the enzyme was layered as monomer. For the data of Table I, the layered volume was 5–10 μL, and the enzyme concentration range was 0.5–1.5 μg/mL.

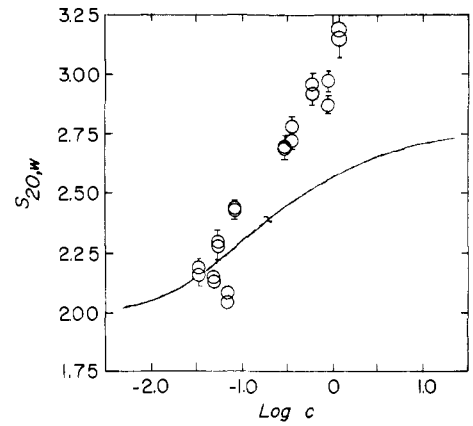

FIGURE 4: Active-enzyme sedimentation of cobra (*Naja naja naja*) venom $PLPA_2$. The ordinate is the observed sedimentation coefficient for the active-enzyme zone corrected to 20 °C in water. The abscissa is the log of the total concentration of layered enzyme in milligrams per milliliter. The substrate is 40 mM diC4PC at pH 8.2 in 0.2 M KCl, 1 mM $CaCl_2$, 0.0014% Cresol Red, and glycylglycine–MES buffer (variable). The solid line is that expected from the thermodynamic studies with K_2 = 10.26 L/g (k_2 = 6.9 × 10^4 L/mol); association constant from monomer to dimer and s(monomer) = 1.98 S.

The final row of Table I gives the result for the sedimentation coefficient when the diC6PC substrate is reduced from 7.5 to 4.0 mM in the active-enzyme sedimentation experiment. The value of 4.68 S indicates polymerization of the enzyme far beyond the dimeric state.

DISCUSSION

It is generally accepted that the active form of the *Crotalus* $PLPA_2$ is the dimer based on the kinetic behavior of the enzyme in lipid monolayers (Shen et al., 1975) and the active-enzyme sedimentation velocity results of Smith and Wells (1981). The active-enzyme gel filtration experiment of Smith and Wells (1981) is inconclusive because the enzyme reaction products do not dissociate the dimer and the flow rate is sufficiently slow on such columns to allow hydrolysis of the substrate. The experiments reported here cast serious doubt on the hypothesis that the dimeric enzyme is the active form.

The elegant experiments of Shen et al. (1975) have been criticized by Volwerk et al. (1979). The criticism is based on observations by Rietsch et al. (1977) that a significant fraction (76%) of radioactive porcine pancreatic $PLPA_2$ was adsorbed to a Teflon apparatus. Thus, enzyme losses by adsorption to the Langmuir trough surface may have played a significant role in the experiments of Shen et al. (1975). In our hands, the $PLPA_2$ enzymes adsorb readily to glass and quartz, requiring detergent scrubbing or a pepsin treatment between enzyme assays. A second problem with the analysis of Shen et al. (1975) is the assumption of pure dimer as an initial boundary condition of the mathematical analysis. It is very difficult to determine whether this assumption is a serious defect or not. Finally, as a further complication of the problem, we observed in this study that the linkage of dimerization to substrate binding and turnover is dependent on the substrate. Almost certainly, the dimerization linkage also depends on whether the substrate is monomeric or aggregated as a monolayer.

We began our studies of active-enzyme centrifugation using the *Crotalus* $PLPA_2$ as a dimeric control for the *Naja* enzyme. Only after many confusing experiments were we led to the possibility of an artifact in the report of Smith and Wells (1981). When we calculated the pH as a function of radial position in the centrifuge cell, the nature of the problem and

Scheme III: *Crotalus* $PLPA_2$ Substrate Linkage

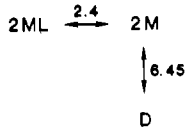

its solution became clear. By the simple expedient of adding the MES buffer to the solution to prevent the leading portion of the enzyme zone from inactivating the trailing region due to lowered pH, the experiments were reproducible and could be performed over a reasonable range of enzyme concentration. The zone sedimentation of *Crotalus* $PLPA_2$ in Sr^{2+} and diC6PC has been an important control in the experiments reported here.

We think that we have eliminated all of the artifacts in the active-enzyme sedimentation results reported here (except those used to illustrate the artifacts). If, for example, a large fraction of the enzyme adsorbed to the epoxy centerpiece, one might expect a decreased sedimentation coefficient to be calculated. Under this circumstance, we would expect to observe a sysematic decrease in activity with time of the experiment, but this is not the case. Exclusive of the first few time points, there was no systematic change from one experiment to another. A small fraction of enzyme adsorbed to the centerpiece should give pH patterns which are the reverse of Figure 3 in the trailing portion of the zone of activity. This is because the enzyme concentration is greatest at the initial layering and decreases substantially as the zone diffuses. An adsorption process should show greatest adsorption at the highest concentration. Since the adsorbed enzyme would have to continue to turn over substrate to cause an artifact, the pH should be lowest at the meniscus and gradually increase toward the active zone, similar to that seen in Figure 2. The zone sedimentations in Sr^{2+} and in Sr^{2+} with diC6PC would also appear to eliminate enzyme adsorption as a possible artifact.

Without further assumptions, the results of this work should not be interpreted as indicating either monomer or dimer is the active species. The data of Figure 1 and Table I indicate that the active species sediments as a reaction boundary. The association of the $PLPA_2$ enzymes in diC4PC appears unaffected by the substrate. The *Crotalus* $PLPA_2$ apparently turns over this substrate as the dimer, but it may be that the small fraction of monomer present in the solution is responsible for the hydrolysis. In the *Naja* $PLPA_2$ active-enzyme sedimentation, the linkage of substrate binding and turnover to dimerization is sufficiently weak that the dimerization constant determined in the absence of substrate adequately describes the active-enzyme sedimentation behavior, at least to a first approximation (Figure 4).

If we assume that only monomer *Crotalus* $PLPA_2$ binds diC6PC, then is is possible to write the linkage Scheme III for the dissociation and compare the consequences of the scheme with the observed results.

In this scheme, the number 2.4 is pK_m, the negative log of the Michaelis constant [from Allgyer & Wells (1979)], while the number for the vertical reaction is taken from Figure 1. In this scheme, L refers to the diC6PC substrate. The appropriate linkage equation is

$$\log k_{2,\text{obsd}} = \log k_{2,L=0} - 2 \log (1 + k_m L) \qquad (9)$$

where k_m is the reciprocal Michaelis constant and L now represents substrate concentration. At $L = 7.5$ mM, $\log k_{2,\text{obsd}}$ is 5.45 from the numbers of the scheme. From the Sr^{2+} with diC6PC experiment of Table I, with the weight fraction of dimer taken as 0.61 ± 0.13 and the enzyme concentration at 0.45 mg/mL, we calculate $\log k_{2,\text{obsd}} = 4.8 \pm 0.4$. The calculation is sufficiently crude and the result sufficiently close to that expected from the scheme to consider that monomeric $PLPA_2$ is the active-enzyme species. In order to entertain this proposal seriously, however, one must first find fault with the very conclusive experiments of Wells (1973) demonstrating half-site reactivity with ethoxyformic anhydride but complete loss of enzyme activity. The modification has been reviewed critically be Verheij et al. (1981), but the criticism should be considered in light of current knowledge of the *Crotalus atrox* structure (Keith et al., 1981; Brunie et al., 1984).

A similar calculation using Scheme III may be made for the diC4PC substrate with $K_m = 32$ mM (Wells, 1972) and $L = 40$ mM. At the enzyme concentration of 0.05 mg/mL, we should have observed 2.5 S ($w_1 = 0.39$). The observed value of 2.77 ± 0.12 S in Table I indicates little or no substrate-linked dissociation for the *Crotalus* $PLPA_2$, however.

With these two calculations, we are led to the conclusion that the *Crotalus* $PLPA_2$ enzyme can act as either monomer or dimer depending on the assay. We speculate that this may be the key point which allows the conflicting observations to be reconciled.

The next problem to address is the apparent association of *Naja* $PLPA_2$ induced by diC6PC. Recent investigations from several laboratories have demonstrated aggregatior of protein–lipid complexes below the critical micelle concentration (van Eijk et al., 1983; van Oort et al., 1985; Plückthun & Dennis, 1985). This phenomenon has been observed with *Naja melanoleuca* $PLPA_2$ (van Eijk et al., 1983), *Naja naja naja* $PLPA_2$ (Plückthun & Dennis, 1985), and porcine pancreatic $PLPA_2$ (van Oort et al., 1985) with a variety of substrates and substrate analogues larger, however, than diC6PC. Since the enzyme concentrations in our active-enzyme experiments were 10^{-7} M and less, it is most reasonable to interpret the sedimentation coefficient of 2.40 S in Table I as a protein–lipid aggregate rather than a self-association process. Since we have no data on the shape of such an aggregate with sedimentation coefficient s_c, we assume its friction will correspond to isomorphous expansion of the monomeric enzyme with sedimentation coefficient s_m. Let us now represent component 2 as protein; component 3 is lipid substrate. Further, assuming constant hydration by component 1 (water and buffer), we can write the following equation for the sedimentation coefficient:

$$s_c/s_m = [M_2(1 - \bar{v}_2\rho) + nM_3(1 - \bar{v}_3\rho)] \times (M_2\bar{v}_2)^{1/3}/[M_2(1 - \bar{v}_2\rho)](M_2\bar{v}_2 + nM_3\bar{v}_3)^{1/3} \qquad (10)$$

In this equation, n is the number of lipid molecules bound to the protein with mass M_2 in grams per mole. The value of M_3 we used was 471.5 g/mol for diC6PC corresponding to the monohydrate, and $\bar{v}_3$ was 0.864 mL/g at 20 °C derived from the results of Tausk et al. (1974). We used the temperature dependence of $\bar{v}_3$ calculated from many literature references on partial molal volumes of detergents and fatty acids as $d\bar{v}_3/dT = 1.3 \times 10^{-3}$ mL g^{-1} deg^{-1}. The first approximation is to simply calculate the value of n for the $s_{20,w}$ value of Table I. This yields $n = 60 \pm 15$ mol of bound diC6PC per mole of monomeric *Naja* $PLPA_2$.

However, the values of $s_{20,w}$ which contributed to the average value were 10 experiments (20 sedimentation coefficients) performed at temperatures between 19.5 and 26 °C. Since the partial specific volume term appears in the correction to 20 °C, the average value of Table I is incorrect. In order to find the correct value of the molecular parameters from these experiments, we corrected the value of s_m to the conditions of the experiment. Of course, $\bar{v}_2$ must also be corrected to the experimental conditions for which we used $d\bar{v}_2/dT = 3.9 \times$

10^{-4} mL g^{-1} deg^{-1} (Pilz & Czerwenka, 1973). Then, n, $\bar{v}_c$, and M_c could be calculated from eq 10 under the experimental conditions. We use the subscript c for the protein–lipid complex. Since $\bar{v}_c$ was now known, the observed sedimentation coefficient could be corrected to 20 °C and water in the usual way. The result was $n = 68 \pm 16$, $s_{c,20,w} = 2.47 \pm 0.14$ S, $\bar{v}_c = 0.808 \pm 0.010$ mL g^{-1}, and $M_c = 45\,700 \pm 7500$ g mol^{-1}.

There is some supporting evidence that this model is on the right track. We have been unable to perform zone sedimentation velocity with the Sr^{2+} and diC6PC at 0.45 mg/mL *Naja* $PLPA_2$ without apparent convection and large sedimentation coefficients in the range of 3.6 S. At such high protein concentration, we should expect aggregation of the protein–lipid complexes. Thirty percent of the total lipid (7.5 mM) would be required to form each complex containing one protein molecule. Also, since the partial molal volume of lipid molecules in micelles is larger than that of the monomeric lipid, pressure dependence of the aggregation would be expected; the leading part of the sedimenting zone showed ripples of optical density as often seen in pressure-dependent associating systems of proteins.

The putative protein–lipid complexes contain about twice the number of diC6PC molecules as are present in the rather narrow molecular weight distribution of pure diC6PC micelles (Tausk et al., 1974). Our calculation of the number of lipid molecules in the complex is only weakly shape dependent. Thus, we expect the complexes to be a simple 1:2 ratio of a protein molecule with two condensed micelles.[2] Indeed, an equilateral triangle of three identical spheres with mass and specific volume of the complex has a calculated sedimentation coefficient of 2.45 S while a linear array of three spheres has 2.30 S [from Swanson et al. (1980)]. Without some detailed friction coefficient measurements on the diC6PC, such sedimentation coefficient calculations must be considered approximations. The model thus suggests that two sites on the enzyme surface interact with a few diC6PC molecules and thus induce micelle formation at these sites. In spite of the large error in n associated with our data, the stoichiometry fits remarkably well. Two micelles would require 34 ± 8 diC6PC molecules. The micelle size reported by Tausk et al. (1974) is 37 ± 5.

The "polymerization" of enzyme activity which is observed when the substrate concentration is lowered to 4.0 mM (Table I) would be due to the association of monomicellar enzyme–lipid complexes. Qualitatively, we anticipate one micelle nucleation site to be more effective than the other; however, the site with no micelle formed associates with a preexisting micelle, thus making a head to tail oligomer much like a polyester condensation reaction.

For a final discussion of the *Naja* $PLPA_2$ active enzyme sedimentation velocity results, we must consider the deviation from thermodynamically predicted sedimentation coefficients in diC4PC that occurs above protein concentrations of 0.1 mg/mL (Figure 4). Since Plückthun and Dennis (1982) have observed a saturable "activator" site with this substrate and enzyme when acting on mixed micelles at 40 °C, our first interpretation of the deviations of the data in Figure 4 was to invoke a linkage of diC4PC with association. While this interpretation gave a better fit to the observed data than the nonlinked curve of Figure 4, significant deviations still occur in the region of 1 mg/mL $PLPA_2$ concentration. In fact, no model in which association proceeds only to the dimer will adequately describe the data. With the discussion of the diC6PC effect on this enzyme above, it is natural to suppose that protein–lipid complexes occur in the diC4PC solutions as well. As protein concentration is increased at constant substrate concentration, any such complexes would be expected to aggregate. The lipid:protein ratio and the total protein concentration would determine whether the complexes aggregate. Unfortunately, since the dimerization of *Naja* $PLPA_2$ occurs significantly at the high concentrations used for the experiments, quantitative analysis is complicated.

One implication of the micellar nucleation model to the enzymology of $PLPA_2$ is that it facilitates the interpretation of the activation of the enzyme by low (7 mM) concentrations of such a poor substrate as diC4PC when the enzyme activity is monitored on phosphatidylethanolamine substrate in mixed micelles (Plückthun & Dennis, 1982). Thus, we would identify one micellar nucleation site with the activator site of these authors.

The diC6PC substrate in the presence of Ca or Sr ion dissociates the *Crotalus* $PLPA_2$ dimer. The experiments reported here cast doubt on the dogma of dimeric *Crotalus* $PLPA_2$ activity but are not conclusive in proving either the monomer or the dimer is the active species on this substrate. We have not yet found a micellar nucleation site on the *Crotalus* $PLPA_2$, but only a few experiments have been performed outside the conditions of Table I so we currently have no information whether this enzyme might show the effect under other pH or substrate conditions. Possibly this enzyme may only influence the diC6PC substrate above the cmc (Allgyer & Wells, 1979; Johnson et al., 1981).

The diC6PC induces an increase in the sedimentation coefficient of the *Naja* $PLPA_2$ monomer, and the diC4PC substrate appears to act similarly at high enzyme:substrate ratios. The interpretation of the results with the diC6PC substrate as a micelle nucleation process fits the available data very well, and the results with the diC4PC substrate are in qualitative agreement with the model.

It is certainly the case that the linkage of activity to association of these enzymes is substrate dependent for such small substrates as used in this study.

ACKNOWLEDGMENTS

We thank Dr. C. de Haën for discussions and Dr. M. A. Wells and Dr. P. Kanda for technical advice; J. W. Godden is thanked for many hours of advice and assistance.

Registry No. $PLPA_2$, 9001-84-7; diC6PC, 63-89-8.

REFERENCES

Aguiar, A., de Haas, G. H., Jansen, E. H. J. M., Slotboom, A. J., & Williams, R. J. P. (1979) *Eur. J. Biochem. 100*, 511–518.

Allgyer, T. T., & Wells, M. A. (1979) *Biochemistry 18*, 4354–4361.

Bernstein, F. C., Koetzle, T. F., Williams, G. J. B., Meyer, E. F., Jr., Brice, M. D., Rodgers, J. R., Kennard, O., Shimanouchi, T., & Tasumi, M. (1977) *J. Mol. Biol. 112*, 535–542.

Brunie, S., Bolin, J., Gewirth, D., & Sigler, P. B. (1985) *J. Biol. Chem. 260*, 9742–9749.

[2] Alternatively, one can achieve approximate agreement of the Stokes radius expansion of the $PLPA_2$ molecule from 19.3 Å for the protein alone to 31.5 Å for the complex by packing the surface with 68 nonoverlapping cylinders of radius 4.0 Å and height 13.5 Å. This calculation was made by packing the bovine $PLPA_2$ X-ray coordinates (Dijkstra et al., 1981; Bernstein et al., 1977) with spheres of various radii and then matching the molecular volume of diC6PC [$V = 4\pi(5.46)^3/3$] to the height of a cylinder of radius 4.0 Å; 68 nonoverlapping spheres of radius 4.0 Å can access the surface of these coordinates. We feel that this model is much less likely than micellar nucleation by a few surface residues.

Cohen, R. (1963) *C. R. Hebd. Seances Acad. Sci. 256*, 3513–3515.
Cohen, R., & Mire, M. (1971) *Eur. J. Biochem. 23*, 267–275.
Darke, P. L., Jarvis, A. A., Deems, R. A., & Dennis, E. A. (1980) *Biochim. Biophys. Acta 626*, 154–161.
Darrow, R. A., & Colowick, S. P. (1962) *Methods Enzymol. 5*, 226–235.
de Haas, G. H., Postema, N. M., Nieuwenhuizen, W., & van Deenen, L. L. M. (1968) *Biochim. Biophys. Acta 159*, 103–117.
de Haën, C., Easterly, R. A., & Teller, D. C. (1983) *Biopolymers 22*, 1133–1143.
Dijkstra, B. W., Kalk, K. H., Hol, W. G. J., & Drenth, J. (1981) *J. Mol. Biol. 147*, 97–123.
Dijkstra, B. W., Renetseder, R., Kalk, K. H., Hol, W. G. J., & Drenth, J. (1983) *J. Mol. Biol. 168*, 163–179.
Efron, B., & Diaconis, P. (1983) *Sci. Am. 248* (*5*), 116–130.
Faxén, H. (1936) *Ark. Mat., Astron. Fys. 25B*, 1.
Fiske, C. H., & Subbarow, Y. (1929) *J. Biol. Chem. 81*, 629.
Fujita, H. (1975) *Foundations of Ultracentrifugal Analysis*, Wiley, New York.
Hoagland, V. D., Jr., & Teller, D. C. (1969) *Biochemistry 8*, 594–602.
Holbrook, J. J., Liljas, A., Steindel, S. J., & Rossman, M. G. (1975) *Enzymes (3rd Ed.) 11A*, 263.
Holcenberg, J. S., Teller, D. C., Roberts, J., & Dolowy, W. C. (1972) *J. Biol. Chem. 247*, 7750–7758.
Johnson, R. E., Wells, M. A., & Rupley, J. A. (1981) *Biochemistry 20*, 4239–4242.
Kanda, P., & Wells, M. A. (1981) *J. Lipid Res. 22*, 877–879.
Keith, C., Feldman, D. S., Deganello, S., Glick, J., Ward, K. B., Jones, E. O., & Sigler, P. B. (1981) *J. Biol. Chem. 256*, 8602–8607.
Kemper, D. L., & Everse, J. (1973) *Methods Enzymol. 27D*, 67–82.
Kornberg, A. (1955) *Methods Enzymol 1*, 441–443.
Lamm, O. (1929) *Z. Phys. Chem., Abt. A 143*, 177.
Landoldt-Börnstein (1977) *Numerical Data and Functional Relationships in Science and Technology, New Series*, Group 4, Vol. 1B, Springer-Verlag, New York.
Lee, A. W., & Karplus, M. (1983) *Proc. Natl. Acad. Sci. U.S.A. 80*, 7055–7059.
Llewllyn, D. J., & Smith, G. D. (1978) *Arch. Biochem. Biophys. 190*, 483–494.
Pilz, I., & Czerwenka, G. (1973) *Makromol. Chem. 170*, 185–190.
Plückthun, A., & Dennis, E. A. (1982) *Biochemistry 21*, 1750–1756.
Plückthun, A., & Dennis, E. A. (1985) *J. Biol. Chem. 260*, 11099–11106.
Renetseder, R., Brunie, S., Dijkstra, B. W., Drenth, J., & Sigler, P. B. (1985) *J. Biol. Chem. 260*, 11627–11634.
Rietsch, J., Pattus, F., Desnuelle, P., & Verger, R. (1977) *J. Biol. Chem. 252*, 4313–4318.
Schwert, G. W., Miller, B. R., & Peanasky, R. J. (1967) *J. Biol. Chem. 242*, 3245–3252.
Senear, D. F., & Teller, D. C. (1981a) *Biochemistry 20*, 3076–3083.
Senear, D. F., & Teller, D. C. (1981b) *Biochemistry 20*, 3083–3091.
Shen, B. W., Tsao, F. H., Law, J. H., & Kézdy, F. J. (1975) *J. Am. Chem. Soc. 97*, 1205–1208.
Smith, C. M., & Wells, M. A. (1981) *Biochim. Biophys. Acta 663*, 687–694.
Swanson, E., Teller, D. C., & de Haën, C. (1980) *J. Chem. Phys. 72*, 1623–1628.
Szabo, A., & Karplus, M. (1972) *J. Mol. Biol. 72*, 163–197.
Szabo, A., & Karplus, M. (1976) *Biochemistry 15*, 2869–2877.
Tausk, R. J. M., van Esch, J., Karmiggelt, J., Voordouw, G., & Overbeek, J. Th. G. (1974) *Biophys. Chem. 1*, 184–203.
Teller, D. C. (1973) *Methods Enzymol. 27D*, 346–441.
Teller, D. C., Swanson, E., & de Haën, C. (1979) *Methods Enzymol. 61H*, 103–124.
van Eijk, J. H., Verheij, H. M., Dijkman, R., & de Haas, G. H. (1983) *Eur. J. Biochem. 132*, 183–188.
van Oort, M. G., Dijkman, R., Hille, J. D. R., & de Haas, G. H. (1985) *Biochemistry 24*, 7987–7993.
Verheij, H. M., Slotboom, A. J., & de Haas, G. H. (1981) *Rev. Physiol., Biochem. Pharmacol. 91*, 91–203.
Volwerk, J. J., Dedieu, A. G. R., Verheij, H. M., Dijkman, R., & de Haas, G. H. (1979) *Recl: J. R. Neth. Chem. Soc. 98*, 214–220.
Wells, M. A. (1971) *Biochemistry 10*, 4078–4083.
Wells, M. A. (1972) *Biochemistry 11*, 1030–1041.
Wells, M. A. (1973) *Biochemistry 12*, 1086–1092.
Wells, M. A. (1975) *Biochim. Biophys. Acta 380*, 501–505.
Wells, M. A., & Hanahan, D. J. (1969) *Biochemistry 8*, 414–424.
Wyman, J. (1964) *Adv. Protein Chem. 19*, 223–286.
Yphantis, D. A. (1964) *Biochemistry 3*, 297–317.